Clay Minerals, (2016) **51**, 69–80

MAS NMR and EPR study of structural changes in talc and montmorillonite induced by grinding

ROGER BORGES[1], LÍVIA MACEDO DUTRA[2], ANDERSSON BARISON[2] AND FERNANDO WYPYCH[1,*]

[1] *CEPESQ – Research Center for Applied Chemistry, Department of Chemistry, Federal University of Paraná - PO Box 19032, Curitiba, PR, 81530-980, Brazil*

[2] *NMR Center, Department of Chemistry, Federal University of Paraná - PO Box 19032, Curitiba, PR, 81530-980, Brazil*

(*Received 20 November 2015; revised 17 March 2016; Editor: George Christidis*)

ABSTRACT: The milling process in the solid-state 2:1 clay minerals, montmorillonite and talc, which have different cation exchange capacities, is reported here. Several instrumental techniques were used to monitor systematically the products formed. The dehydroxylation/amorphization of the montmorillonite and talc structures occurs within 3 and 6 h of milling, respectively. Electron paramagnetic resonance spectra indicated that structural Mn^{2+} was oxidized more quickly in the montmorillonite structure than in talc, while the paramagnetic defects increased during milling. Nuclear magnetic resonance was also used to monitor the environmental changes for Si and Al during milling.

KEYWORDS: mechanochemical activation, 2:1 clay minerals, redox reactions, MAS NMR, EPR.

Solid-state mechanochemical activation of materials includes milling to increase their reactivity, allows reactions in the solid state and decreases the decomposition temperature, causing structural defects and structural transformation, formation of metastable amorphous or hybrid materials, *etc.* (Mingelgrin *et al.*, 1978; Garcia *et al.*, 1991; Sanchez-Soto *et al.*, 1997; Mendelovici, 2001; Christidis *et al.*, 2004, 2005; Dellisanti & Valdré, 2005; Balek *et al.*, 2007, 2008; Ramadan *et al.*, 2010; Vizcayno *et al.*, 2010; Djukic *et al.*, 2013; Dumas *et al.*, 2013; Galimberti *et al.*, 2014; Petra *et al.*, 2015). One of the applications of this process is to obtain material for sustainable slow-release fertilizers (Zhang *et al.*, 2009; Solihin *et al.*, 2010, 2011), by combining an insoluble clay mineral and a soluble phosphate, yielding phases with low solubility. The effectiveness depends mainly on stoichiometric proportions of the materials used, time and energy of milling.

The mechanisms of this process and the chemical composition of the slightly soluble materials obtained were elucidated mainly with the use of solid-state nuclear magnetic resonance (NMR) spectra (Borges *et al.*, 2015). Redox reactions and the formation of free radicals still require explanation, however. Electron paramagnetic resonance (EPR) enables investigation of these phenomena as well as the identification of inorganic radicals, because it is highly sensitive to paramagnetic species such as Fe^{3+} and Mn^{2+} (Kudynska *et al.*, 1989; Siqueira *et al.*, 2011). These species often occur as minor elements at low concentrations substituting for the main components in the structures of the clay minerals.

The present study reports the effects of milling on structural changes in raw montmorillonite and talc as potential matrices to obtain sustainable slow-release

*E-mail: wypych@ufpr.br
DOI: 10.1180/claymin.2016.051.1.06

fertilizer. Both are 2:1 layer silicates. The main objective is to investigate the redox reactions and structural changes induced by milling. In addition to having different chemical compositions, montmorillonite is a cation exchanger while talc does not have layer charge. However, both have isomorphic paramagnetic species substituting for structural cations, mainly in the octahedral sheet, which can be monitored by EPR. This technique was used to monitor the changes to these paramagnetic species during the milling process.

MATERIALS AND METHODS

Montmorillonite (SWy-2 – $(Ca_{0.12}Na_{0.32}K_{0.05})[Al_{3.01}Fe^{(III)}_{0.41}Mn_{0.01}Mg_{0.54}Ti_{0.02}][Si_{7.98}Al_{0.02}]O_{20}(OH)_4$) was obtained from the Source Clays Repository of The Clay Minerals Society, while the commercial talc (idealized formula – $Mg_3Si_4O_{10}(OH)_2$) was obtained from the company Magnesita, in Brazil.

Experimental

The solid-state mechanochemical reactions were performed using 1 mmol of each clay mineral, at 70 rpm ($0.2876 \times g$). The montmorillonite was ground for 3, 6 and 9 h and talc, being more resistant to the milling process, was milled for 6, 9 and 12 h. All reactions were performed using a mortar Fritsch Pulverisette 2 grinder, consisting of a zirconium vessel with 10.5 cm diameter and zirconium disk attached to the mill by a fixing rod.

The samples had previously been placed in a closed chamber for a week, under controlled humidity of 40%, and the hygroscopic moisture content was measured in a Shimadzu MOC63u moisture balance, with straight type halogen heater.

Fourier transform infrared (FTIR) spectra were obtained in a Bio-Rad FTS 3500GX FTIR spectrometer with an accumulation of 32 scans, a resolution of 4 cm^{-1}, employing KBr tablets at a mass ratio of 1:100 (sample:KBr). Thermogravimetric analysis (TGA) curves were obtained for the samples and reagents, with a Mettler Toledo TG/s DTA 851 E analyser, using 150 μL alumina crucibles and a temperature ramp of 10°C min^{-1}, under oxygen flow of 50 mL min^{-1}.

The EPR spectra were obtained at ambient temperature (~25°C) in a Bruker EMX spectrometer operating at X-band (~9.5 GHz) employing a 100 kHz modulation frequency and 5000 G of amplitude modulation. The NMR spectra in solid form were acquired using a Bruker AVANCE 400 spectrometer operating at 9.4 Tesla, to observe ^{27}Al and ^{29}Si nuclei at 104.2 and 79.5 MHz, respectively, equipped with a 4 mm multinuclear solids probe and spinning at the magic angle at 5000 Hz. The MAS NMR spectra of ^{27}Al were acquired from 32 K points, 1 K scans, by applying 90° excitation pulses and a relaxation time of 1 s. On the other hand, the spectra of ^{29}Si MAS NMR were acquired from 32 K points, 2 K scans, by applying a 15° excitation pulse and a relaxation time of 5 s. The spectra were processed by applying an exponential multiplication in Free Induction Delays (FIDs) by factors of 200 and 100 Hz, respectively, followed by Fourier-transform for completion to 64 K points. To observe the percentage of individual species, the ^{29}Si NMR spectra were deconvoluted, whereas ^{27}Al spectra were integrated.

Nitrogen adsorption isotherms were obtained with a Quantachrome NOVA 2000e gas sorption analyser. The samples were preheated at 100°C under vacuum for 2 h and were subjected to analysis at 77 K. The specific surface areas of the samples were calculated using the multi-point Brunauer-Emmet-Teller (BET) method.

RESULTS AND DISCUSSION

The X-ray diffraction (XRD) patterns showed that the amorphization of the montmorillonite and talc structures occurs within 3 and 6 h of milling, respectively. After these milling times, only the characteristic peaks of quartz (Q), a natural mineral contaminant in clays, were observed (Boulingui *et al.*, 2015). Quartz resists the milling process (Fig. 1A,B).

The main interest in obtaining amorphous metastable structures from clay minerals is that they tend to be more reactive than their crystalline counterparts, allowing the establishment of bonds with other reagents such as phosphates. When layered hydroxide structures are ground, they collapse mainly due to friction forces; dehydroxylation reactions occur and mixtures of nanostructured oxides are obtained, with highly structural defects. As a result, a gradual reduction in diffraction maxima caused by increasing milling time is observed (Aglietti & Lopez, 1991; Hrachova *et al.*, 2007; Ramadan *et al.*, 2010; Dellisanti *et al.*, 2011).

Although XRD patterns provide important information about the nature of structural modifications, the mechanochemical dehydroxylation process may be confirmed by FTIR and other instrumental techniques.

In the FTIR spectra of the montmorillonite milled for 3 h, a broad band was observed in the range

https://doi.org/10.1180/claymin.2016.051.1.06 Published online by Cambridge University Press

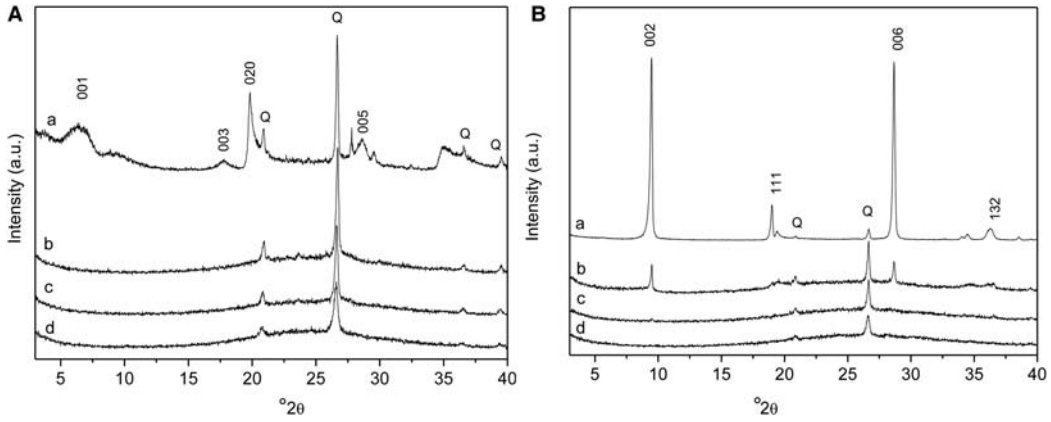

FIG. 1. XRD patterns of raw montmorillonite (A-a) and after milling for 3 h (A-b), 6 h (A-c), 9 h (A-d); raw talc (B-a) and after milling for 6 h (B-b), 9 h (B-c) and 12 h (B-d).

3700–3000 cm^{-1} (Fig. 2Ab), replacing the sharp and well-defined bands in the clay mineral spectra of the raw clay (3635, 3400 and 3160 cm^{-1}), which are attributed to (Al,Mg)-OH stretching (3635 cm^{-1}) and H-O-H stretching of water, (Fig. 2Aa) (Kinninmonth *et al.*, 2013; Çelik & Önal, 2014).

In the FTIR spectra of talc, changes were verified after 6 h of milling (Fig. 2Bb), in accordance with the XRD data (Fig. 1B). The bands at 3676 and 670 cm^{-1}, characteristic of Mg–OH bonds, disappear completely, suggesting dehydroxylation during milling (Du & Yang, 2009; Ptáček *et al.*, 2013). For both samples the bands at ~1000 cm^{-1}, characteristic of Si–O stretching, became broader due to a higher degree of chemical heterogeneity caused by the amorphization process. Likewise, the bands at ~520 cm^{-1} and 465 cm^{-1} for montmorillonite and 465 cm^{-1} and 470 cm^{-1} for talc, related to Al–Si–O and Si–O–Si bonds, respectively, became broader with increasing milling time. In general, changes in the spectra, of both montmorillonite and talc, were observed after milling, suggesting the tendency of montmorillonite and talc to form amorphous phases as already observed by XRD.

The TGA curve of the raw montmorillonite showed two mass-loss events, the first up to 100°C, associated with the removal of physisorbed water and water coordinated to the interlayer cations (7% moisture up to 400°C), and the other in the range 600–700°C, associated with structural dehydroxylation (total weight loss = 11.53% at 1000°C) (Fig. 3A).

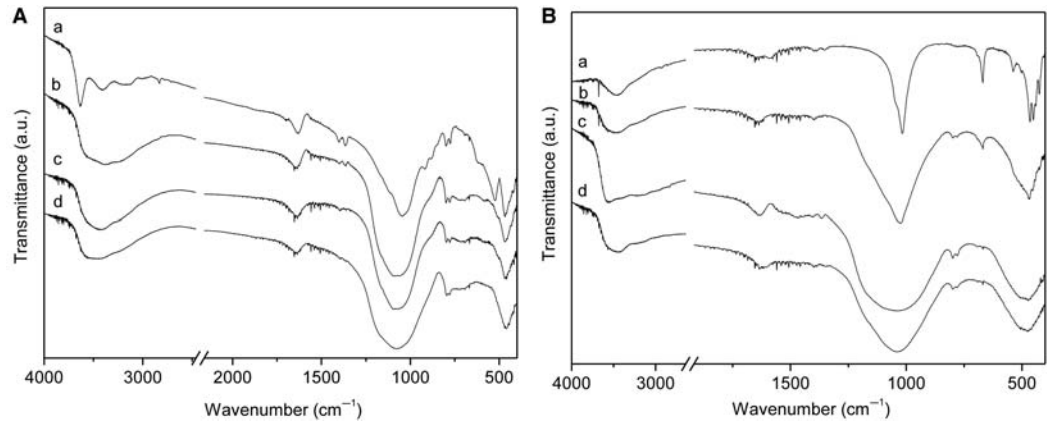

FIG. 2. FTIR spectra of raw montmorillonite (A-a) and after milling for 3 h (A-b), 6 h (A-c) and 9 h (A-d); and of raw talc (B-a) and after milling for 6 h (B-b), 9 h (B-c) and 12 h (B-d).

https://doi.org/10.1180/claymin.2016.051.1.06 Published online by Cambridge University Press

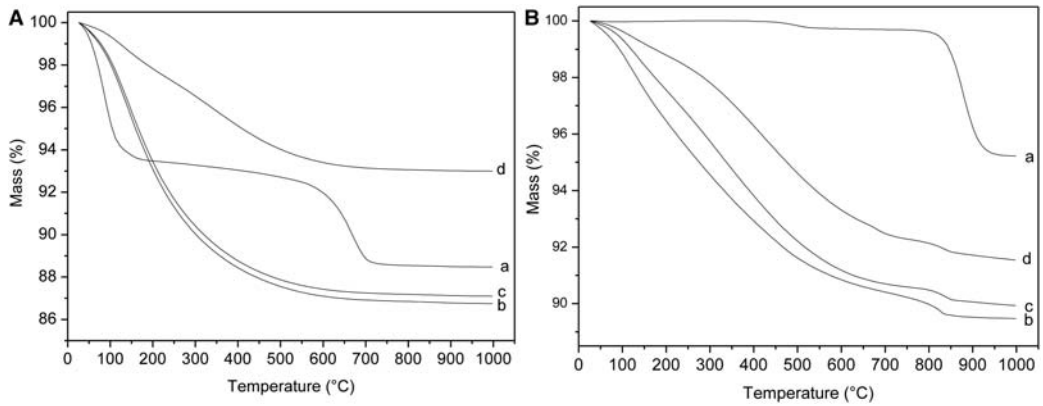

FIG. 3. TGA curves of raw montmorillonite (A-a) and after milling for 3 h (A-b), 6 h (A-c) and 9 h (A-d); and of raw talc (B-a) and after milling for 6 h (B-b); 9 h (B-c) and 12 h (B-d).

In the TGA curves of the milled samples involving montmorillonite, a single weight-loss step was observed from room temperature up to ~700°C. This mass-loss event indicated that mechanochemical dehydroxylation had occurred, as was also shown by FTIR measurements (Fig. 2Ab), because no evidence of thermal dehydroxylation was observed in the TGA curves.

As expected, talc was substantially anhydrous (0.3% mass loss up to 600°C) and a mass loss event of 4.78% occurred at between 800 and 900°C (Fig. 3Ba), in accordance with the theoretical weight loss predicted from the structural formula (4.75%), suggesting that the talc used was of high purity. Although the milled talc samples showed similar thermal profiles to their milled montmorillonite counterparts, even after milling for 9 h (Fig. 2Bd), it was possible to identify a small, sharp mass loss in the region of 800°C, characteristic of thermal dehydroxylation or the formation of a new phase such as orthorhombic enstatite ($MgSiO_3$) (Sanchez-Soto *et al.*, 1997).

In the raw montmorillonite sample (Fig. 4A), the DTG peaks were observed at ~83°C and ~673°C; the first peak was shifted to higher temperatures in the ground materials, whereas the second peak, related to dehydroxylation, disappeared. The displacement of the first peak to higher temperatures may be attributed to the adsorption of water molecules in the amorphous structures which are difficult to release. In the DTG curve of the sample ground for 9 h (Fig. 4Ad), an event was observed at ~379°C, probably related to the mass loss of some amorphous material susceptible to decomposition, probably a carbonate.

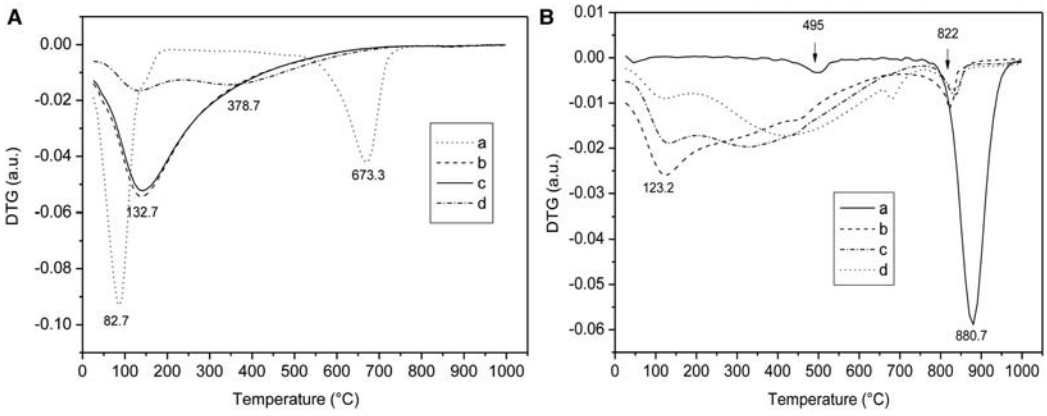

FIG. 4. DTG curves of raw montmorillonite (A-a) and after milling for 3 h (A-b), 6 h (A-c), 9 h (A-d); raw talc (B-a) and after milling for 6 h (B-b); 9 h (B-c) and 12 h (B-d).

https://doi.org/10.1180/claymin.2016.051.1.06 Published online by Cambridge University Press

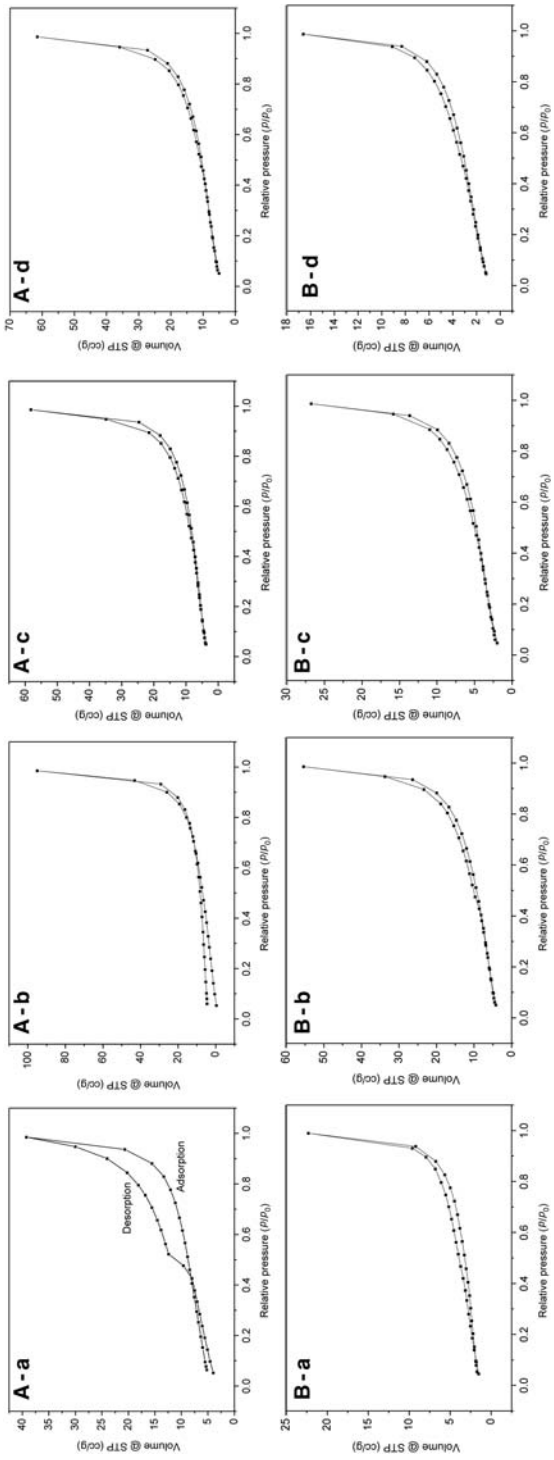

FIG. 5. Adsorption and desorption nitrogen isotherms of raw montmorillonite (Aa) and after milling for 3 h (A-b), 6 h (A-c) and 9 h (A-d); and of raw talc (B-a) and after milling for 6 h (B-b), 9 h (B-c) and 12 h (B-d).

https://doi.org/10.1180/claymin.2016.051.1.06 Published online by Cambridge University Press

Table 1. Textural properties of the montmorillonite and talc samples.

Sample	Milling time (h)	Specific surface area[a] ($m^2\ g^{-1}$)	Pore volume ($cm^3\ g^{-1}$)	Average pore radius (Å)
Montmorillonite	Raw	11.0	0.05443	15.4
	3	17.1	0.14500	29.4
	6	14.9	0.08701	15.3
	9	16.8	0.08994	15.4
Talc	Raw	5.7	0.03331	17.3
	6	17.3	0.08264	15.4
	9	7.6	0.03896	19.3
	12	5	0.02420	17.1

In the raw talc sample, the DTG curves showed peaks at ~495 and ~881°C (Fig. 4Ba) because the milled samples exhibited a more complex superposition of mass-loss events. These events are comparable to those observed for montmorillonite.

The N_2-adsorption curves of raw montmorillonite can be classified according to the IUPAC as type IV, indicating mesoporous materials characterized by capillary condensation in the pores (Fig. 5A). The milled samples showed type III isotherms related to non-porous or macroporous solids, with adsorbate–adsorbate interactions. However, despite the differences in N_2 adsorption and desorption isotherms, all samples showed H4-type hysteresis according to IUPAC classification, which can be related to the narrow slit-pore type.

The increase in the specific surface area (SSA) of the samples compared to the raw montmorillonite may be explained by the reduction in the particle size of the milled material (Table 1). In addition, the volume and average pore radius of montmorillonite milled for 3 h were approximately double that of the raw mineral; however, the average pore radius after 6 h is comparable to the original size. It is suggested that the change in the pore size may be influenced by the formation of amorphous species, and the increase in matrix disorder.

Unlike montmorillonite, the isotherms of the raw and milled talc samples were all of type III with H4-type hysteresis (Fig. 5B). Similar to the montmorillonite samples, the isotherms indicate the existence of non-porous or macroporous materials with relevant adsorbate–adsorbate interactions and narrow slit-type pores.

The sample milled for 3 h had a specific surface area (SSA) which was about three times greater than that of the raw talc, decreasing for longer milling times (Table 1). The sample milled for 12 h had a smaller SSA than the raw clay. This behaviour, as discussed previously, may suggest the formation of amorphous material; the hygroscopic (adsorbed) water study below may also support the discussion on these modifications.

Table 2. Moisture contents of the raw montmorillonite and talc and of the treated samples.

Sample	Milling time (h)	% hygroscopic moisture (average ± standard deviation)
Montmorillonite	Raw	3.30 ± 0.19
	3	2.09 ± 0.23
	6	1.77 ± 0.19
	9	1.31 ± 0.28
Talc	Raw	0.62 ± 0.14
	6	1.47 ± 0.23
	9	1.13 ± 0.23
	12	1.13 ± 0.21

In the case of montmorillonite, in order to examine the effect of milling on the clay's ability to absorb water as qualitative evidence of the presence of hydroxyl groups, the hygroscopic water content decreased with increasing milling time (Table 2). This behaviour may be associated with the mechanochemical dehydroxylation of the mineral matrix. It is suggested that through this process the bound hydroxyls of the clay mineral can react with each other, forming water molecules, thereby reducing the amount of hydroxyl functional groups, which in turn reduces the water-adsorption capacity by hydrogen bonding. Similarly, in the case of talc, the

https://doi.org/10.1180/claymin.2016.051.1.06 Published online by Cambridge University Press

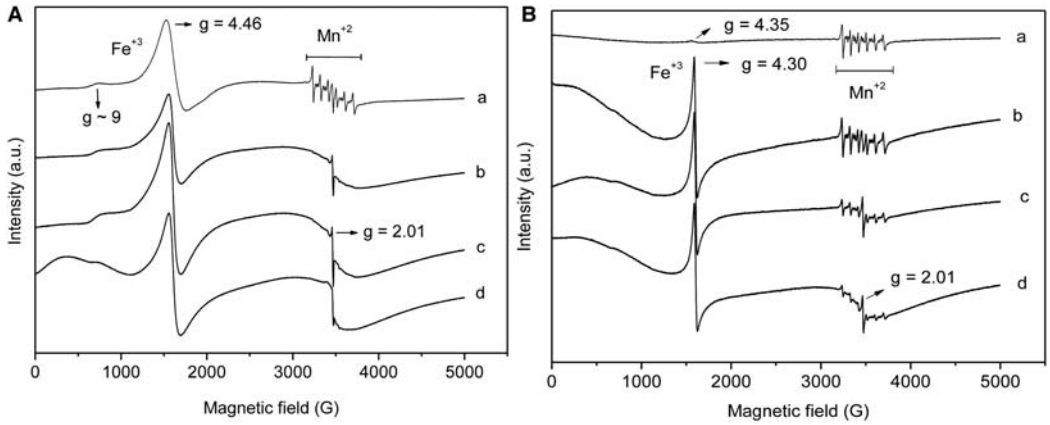

FIG. 6. EPR spectra of raw montmorillonite (A-a) and after milling for 3 h (A-b), 6 h (A-c) and 9 h (A-d); and of raw talc (B-a) and after milling for 6 h (Bb), 9 h (B-c) and 12 h (B-d).

hygroscopic water content increased after the mechanochemical treatment, with the sample milled for 3 h reaching a maximum, after which the water content decreased, becoming constant after ~9 h of milling (Table 2). This behaviour suggests that in the case of talc, the mechanochemical dehydroxylation does not occur directly, but possibly (as discussed in the BET results) there are intermediate structures still containing large proportions of hydroxyl groups. It is considered that after the initial milling, the layered crystals delaminate or break perpendicularly, which ultimately exposes a larger number of hydroxyls, increasing the interaction of the sample with water molecules. A second step occurs with increasing milling time, at which, although dehydroxylation predominates, it is not complete.

Previous work has shown the presence of isomorphic substitutions in clay minerals involving Fe^{3+} and Mn^{2+} (Reddy *et al.*, 2008). These structural paramagnetic species may provide further relevant information about the intermediary species formed during the mechanochemical treatment. To study this aspect, EPR is a very sensitive technique and could be used to trace the evolution of the mechanochemical reaction.

The EPR spectrum of the raw montmorillonite (Fig. 6A), has signals at $g \approx 9$ and $g = 4.5$, characteristic of Fe^{3+} in distorted rhombic sites, and also six

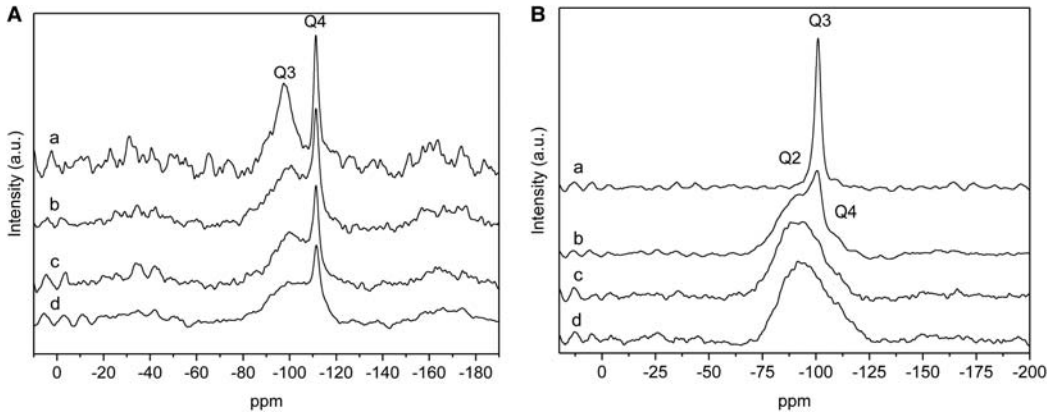

FIG. 7. ^{29}Si MAS NMR spectra of raw montmorillonite (A-a) and after milling for 3 h (A-b), 6 h (A-c) and 9 h (A-d); and of raw talc (B-a) and after milling for 6 h (B-b), 9 h (B-c) and 12 h (B-d).

https://doi.org/10.1180/claymin.2016.051.1.06 Published online by Cambridge University Press

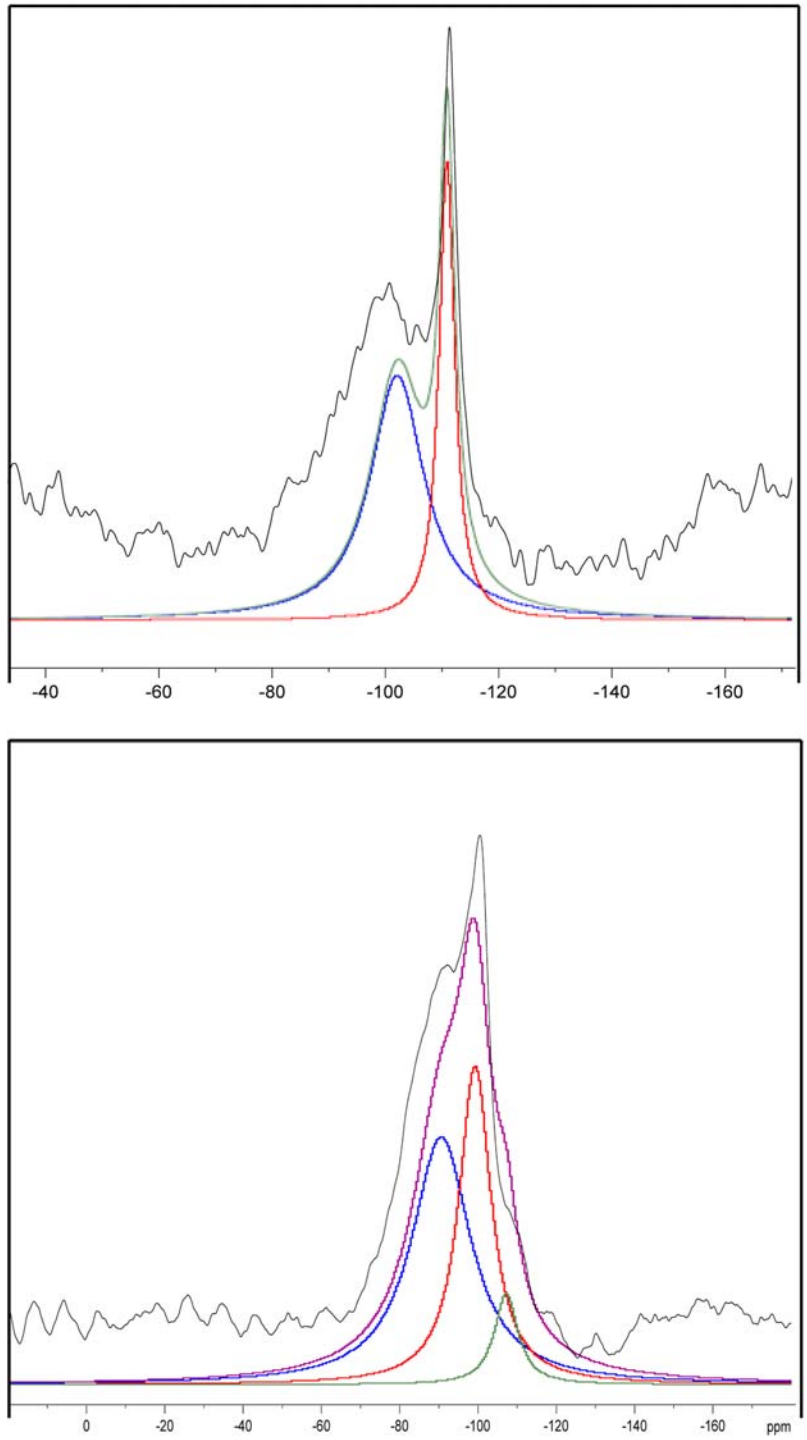

FIG. 8. Deconvoluted ^{29}Si MAS NMR spectra of montmorillonite after milling for 3 h (upper) and of talc after milling for 6 h (lower).

https://doi.org/10.1180/claymin.2016.051.1.06 Published online by Cambridge University Press

TABLE 3. Percentage of different Si sites in the raw and milled samples.

Samples	Mill time (h)	$\%Q^2$	$\%Q^3$	$\%Q^4$
Montmorillonite	Raw	0	65.09	34.91
	3	0	64.78	35.22
	6	0	63.17	36.83
	9	0	59.29	40.71
Talc	Raw	0	100.00	0
	6	54.07	38.04	7.89
	9	32.73	62.05	5.22
	12	29.45	57.12	13.43

lines between g = 2.2 and 1.9, assigned to structural Mn^{2+} (Reddy *et al.*, 2008; Padlyak *et al.*, 2010).

After 3 h of milling, only the signals of Fe^{3+} were observed whereas there is no evidence of Mn^{2+}. It is considered that Mn^{2+} undergoes a mechanochemical oxidation reaction (Fuentes & Takacs, 2013), which may be explained by the occurrence of high-temperature microspots during milling (Lefebvre *et al.*, 2012). The probable product is γ-Mn_2O_3, formed by the oxidation and dehydration of $Mn(OH)_2$ (Greenwood & Earnshaw, 1997). The signal at g = 2.01, which was also present in the raw clay mineral, refers to the structure of oxygen-based free radicals. However, the EPR spectra of the talc samples showed behaviour which was different from that of montmorillonite. The signal of Fe^{3+} was not as obvious at $g \approx 4.4$ in the spectrum (Fig. 6B). It is considered that although the concentration of Fe^{3+} is very low and it exists at the crystal edges, there may exist more abundant Fe^{2+}, which is EPR-silent. During the mechanochemical treatment, Fe^{2+} oxidizes to Fe^{3+}, as was shown by the EPR signal. In contrast, oxidation of Mn^{2+} was not observed, as was the case for montmorillonite. This means that the species of Mn^{2+} are preserved in their raw structure even after milling, in accordance with the TGA results, indicating partial preservation of the talc structure. The signal at g = 2.01 was not apparent in the raw clay mineral, *i.e.* there were no signals relating to defects in the structure in the magnetic resonance. However, after 3 h of milling, the spectra showed this signal, indicating the strong influence of mechanochemical activation in generating free radicals.

In the NMR spectra, the chemical shift depends mainly on the electron density of the nucleus being observed; therefore it is related directly to the donor or withdrawing ligands' capacity coordinated to this nucleus and its coordination number (Guarino *et al.*, 1997).

In Fig. 7A, the montmorillonite sample showed signals in the ^{29}Si MAS NMR spectra at ~–96 ppm

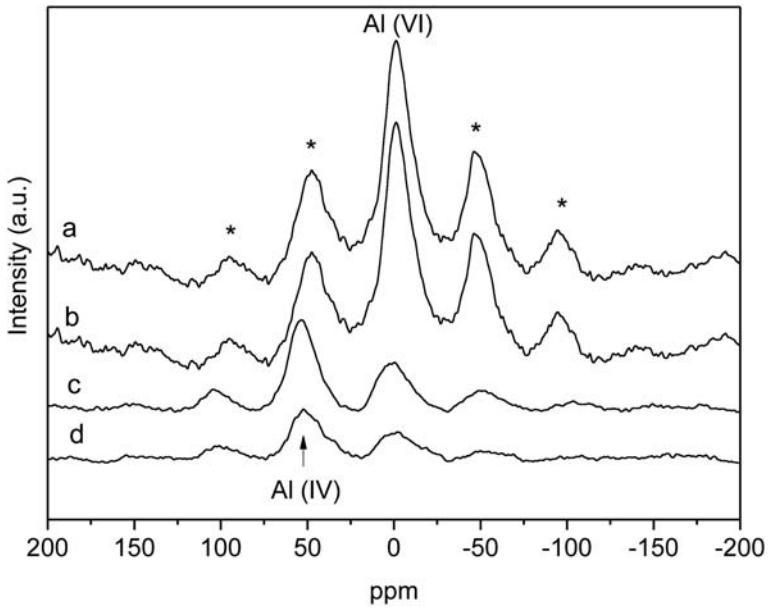

FIG. 9. ^{27}Al MAS NMR spectra of raw montmorillonite (a) and milled for 3 h (b), 6 h (c) and 9 h (d). * Side rotating bands.

https://doi.org/10.1180/claymin.2016.051.1.06 Published online by Cambridge University Press

and –110 ppm, where silicon atoms are bonded to oxygen atoms, characteristic of 2:1 aluminosilicates (Q^3) ($Si(OSi)_3OM$; M = metal) or three-dimensional structures (Q^4) ($[Si(OSi)_4]$), characteristic of quartz present as an impurity (He *et al.*, 2005). After milling the montmorillonite sample the signals remained unaffected, indicating that the same sites were still present. However, the Q^3 signal increased in intensity, probably due to amorphization of the clay mineral structure possibly consisting of several species (Fig. 7A). Moreover, the same level of organization was maintained for the signal attributed to quartz, regardless of the milling time, as already demonstrated by XRD (Fig. 1A).

The ^{29}Si MAS NMR spectrum of talc only had a signal at –96 ppm, related to the Q^3 sites (Fig. 7B) (Martin *et al.*, 2006). The NMR spectra of the samples subjected to milling showed a gradual disruption of the structure and the formation of new sites. Due to the lower concentration of quartz in the sample before milling, the signal at –110 ppm was not detected and the new signals detected at ~–91.0 and –110 ppm, are related to Q^2 ($Si(SiO)_2(OH)_2$) and Q^4 sites, respectively (Coelho *et al.*, 2008). The deconvoluted ^{29}Si MAS NMR spectra of montmorillonite milled for 3 h and talc milled for 6 h can be seen in Fig. 8.

In the milled montmorillonite, the signal attributed to the Q^3 sites was reduced from 65.09% to 59.29%, whereas that of the Q^4 sites increased from 34.91 to 40.71% (Table 3). In the case of talc, the percentage of the Q^3 sites of raw sample was reduced from 100 to 57.12% (Table 3) while that of the Q^2 sites increased from zero to 54.07% for the sample milled for 6 h and then was reduced progressively for samples milled for longer times, reaching 29.45% after milling for 12 h.

The disorganization of the Q^3 site of the montmorillonite caused by milling as indicated in the ^{29}Si MAS NMR spectra (Figs 7, 8) may imply a change in the coordinated AlO_6 octahedral arrangement, because the Q^3 site is coordinated with Al. This change is confirmed in the ^{27}Al MAS NMR spectra by the appearance of the signal at 54.1 ppm corresponding to tetrahedral Al (Fig. 9) in ground samples and the signal at –1.70 ppm attributed to octahedral Al (Isobe *et al.*, 2003; O'Dell *et al.*, 2007; Vyalikh *et al.*, 2009). The NMR spectra indicate a greater number of sites with amorphous Si species and changes in the chemical environment of Al sites after milling. Some of these Si sites resemble amorphous SiO_2, which might improve the reactivity of the ground clay minerals.

Table 4 lists the abundance of Al in different sites of raw and milled montmorillonite samples. The Al sites are transformed from six-fold coordinated (reduced from 100 to 35.4%) to four-fold coordinated (increased from zero to 64.60%), and these data are consistent with the ^{29}Si MAS NMR spectra.

Table 4. Proportions of aluminium in the montmorillonite samples.

Samples	Milling time (h)	$\%Al^{IV}$	$\%Al^{VI}$
Montmorillonite	Raw	0	100.00
	3	64.65	35.35
	6	64.60	35.40
	9	70.08	29.92

CONCLUSIONS

Investigation of mechanochemical processes by traditional techniques such as XRD, FTIR and TGA/DTA, although very important in our understanding of the chemical and physical changes in samples, do not provide adequate evidence about the mechanism of the reaction and the type of chemical environment. This information is extremely important for the synthesis of new structures, and the detection of potential interactions with other ions, *i.e.* phosphates. Hence, characterization by NMR MAS may provide detailed information about the raw species and those formed by the milling process. In addition, the EPR results indicated that the mechanochemical process is oxidizing as a consequence of physical and chemical solid-state reactions. Use of EPR also allowed the identification of defects and the behaviour of paramagnetic species in the samples.

ACKNOWLEDGEMENTS

The authors acknowledge the Brazilian research agencies CNPq, CAPES and FINEP, project Nennan (Fundação Araucária/CNPq), for financial support of this work. RB thanks Ciências sem Fronteiras/CNPq and CNPq for the doctoral grant and LMD thanks CAPES for the doctoral grant.

REFERENCES

Aglietti E.F. & Lopez J.M.P. (1992) Physicochemical and thermal-properties of mechanochemically activated talc. *Materials Research Bulletin*, **27**, 1205–1216.

https://doi.org/10.1180/claymin.2016.051.1.06 Published online by Cambridge University Press

Balek V., Perez-Maqueda L.A.P., Poyato J., Cerny Z., Valle V.R., Buntseva I.M. & Perez-Rodriguez J.L.P. (2007) Effect of grinding on thermal reactivity of ceramic clay minerals. *Journal of Thermal Analysis and Calorimetry*, **88**, 87–91.

Balek V., Perez-Maqueda L.A.P., Benes M., Buntseva I.M., Beckman I.N. & Perez-Rodriguez J.L.P. (2008) Thermal behavior of ground talc mineral. *Journal of Mining and Metallurgy Section B – Metallurgy*, **44**, 7–17.

Borges R., Brunatto S.F., Leitão A.A., Carvalho G.S.G. & Wypych F. (2015) Solid-state mechanochemical activation of clay minerals and soluble phosphate mixtures to obtain slow-release fertilizers. *Clay Minerals*, **50**, 153–162.

Boulingui J.E., Nkoumbou C., Njoya D., Thomas F. & Yvon J. (2015) Characterization of clays from Mezafe and Mengono (Ne-Libreville, Gabon) for potential uses in fired products. *Applied Clay Science*, **115**, 132–144.

Çelik M. & Önal M. (2014) Polythiophene/Na-montmorillonite composites via intercalative polymerization. *Journal of Thermoplastic Composite Materials*, **27**, 145–159.

Christidis G.E., Makri P. & Perdikatsis V. (2004) Influence of grinding on the structure and colour properties of talc, bentonite and calcite white fillers. *Clay Minerals*, **39**, 163–175.

Christidis G.E., Dellisanti F., Valdre G. & Makri P. (2005) Structural modifications of smectites mechanically deformed under controlled conditions. *Clay Minerals*, **40**, 511–522.

Coelho C., Azais T., Bonhomme C., Coury L.B., Boissière C., Laurent G. & Massiot D. (2008) Efficiency of dipolar and J-derived solid-state NMR techniques for a new pair of nuclei $\{^{31}P,^{29}Si\}$. Towards the characterization of Si-O-P mesoporous materials. *Comptes Rendus Chimie*, **11**, 387–397.

Dellisanti F. & Valdre G. (2005) Study of structural properties of ion treated and mechanically deformed commercial bentonite. *Applied Clay Science*, **28**, 233–244.

Dellisanti F., Minguzzi V. & Valdrè G. (2011) Mechanical and thermal properties of a nanopowder talc compound produced by controlled ball milling. *Journal of Nanoparticle Research*, **13**, 5919–5926.

Djukic A., Jovanovic U., Tuvic T., Andric V., Novakovic J.G., Ivanovic N. & Matovic L. (2013) The potential of ball-milled Serbian natural clay for removal of heavy metal contaminants from wastewaters: Simultaneous sorption of Ni, Cr, Cd and Pb ions. *Ceramics International*, **39**, 7173–7178.

Du C. & Yang H. (2009) Simple synthesis and characterization of nanoporous materials from talc. *Clays and Clay Minerals*, **57**, 290–301.

Dumas A., Martin F., Le Roux C., Micoud P., Petit S., Ferrage E., Brendlé J., Grauby O. & Hooper M.G. (2013) Phyllosilicates synthesis: a way of accessing edges contributions in NMR and FTIR spectroscopies. Example of synthetic talc. *Physics and Chemistry of Minerals*, **40**, 361–373.

Fuentes A.F. & Takacs L. (2013) Preparation of multicomponent oxides by mechanochemical methods. *Journal of Materials Science*, **48**, 598–611.

Galimberti M., Coombs M., Cipolletti V., Spatola A., Guerra G., Lostritto A., Giannini L., Pandini S. & Riccò T. (2014) Delaminated and intercalated organically modified montmorillonite in poly(1,4-cis-isoprene) matrix. Indications of counterintuitive dynamic-mechanical behavior. *Applied Clay Science*, **97–98**, 8–16.

Garcia F.G., Abrio M.T.R. & Rodriguez M.G. (1991) Effects of dry milling on two kaolins of different degrees of crystallinity. *Clay Minerals*, **26**, 549–565.

Greenwood N.N. & Earnshaw A. (1997) *Chemistry of the Elements*. Elsevier, Amsterdam, Butterworth-Heinemann, London.

Guarino A.W.S., Gil R.A.S., Polivanov H. & Menezes S. M.C. (1977) Characterization of a Brazilian smectite by solid state NMR and X-ray diffraction techniques. *Journal of the Brazilian Chemical Society*, **8**, 581–586.

He H., Duchet J., Galy J. & Gerard J. (2005) Grafting of swelling clay materials with 3-aminopropyltriethoxysilane. *Journal of Colloid and Interface Science*, **288**, 171–176.

Hrachova J., Komadel P. & Fajnor V.S. (2007) The effect of mechanical treatment on the structure of montmorillonite. *Materials Letters*, **61**, 3361–3365.

Isobe T., Watanabe T., Cailliere J.B.E., Legrand A.P. & Massiot D. (2003) Solid-state ^{1}H and ^{27}Al NMR studies of amorphous aluminum hydroxides. *Journal of Colloid and Interface Science*, **261**, 320–324.

Kinninmonth M.A., Liauw C.M., Verran J., Taylor R., Edwards-Jones V., Shaw D. & Webb M. (2013) Investigation into the suitability of layered silicates as adsorption media for essential oils using FTIR and GC-MS. *Applied Clay Science*, **83–84**, 415–425.

Kudynska J., Duczmal T. & Buckmaster H.A. (1989) Temperature- and time-stability study of the dehydration mechanisms in Ca-montmorillonite – an EPR study. *Applied Clay Science*, **4**, 225–233.

Lefebvre A., Lanzetta F., Lipinski P. & Torrance A.A. (2012) Measurement of grinding temperatures using a foil/workpiece thermocouple. *International Journal of Machine Tools and Manufacture*, **58**, 1–10.

Martin F., Ferrage E., Petit S., Parseval P., Delmotte L., Ferret J., Arseguel D. & Salv S. (2006) Fine-probing the crystal-chemistry of talc by MAS-NMR spectroscopy. *European Journal of Mineralogy*, **18**, 641–651.

Mendelovici E. (2001) Selective mechanochemical reactions on dry milling structurally different silicates. *Journal of Materials Science Letters*, **20**, 81–83.

Mingelgrin U., Kliger L., Gal M. & Saltzman S. (1978) The effect of milling on the structure and behavior of bentonites. *Clays and Clay Minerals*, **26**, 299–307.

https://doi.org/10.1180/claymin.2016.051.1.06 Published online by Cambridge University Press

O'Dell L.A., Savin S.L.P., Chadwick A.V. & Smith M.E. (2007) A ^{27}Al MAS NMR study of a sol-gel produced alumina: Identification of the NMR parameters of the γ-Al_2O_3 transition alumina phase. *Solid State Nuclear Magnetic Resonance*, **31**, 169–173.

Padlyak B.V., Wojtowicz W., Adamiv V.T., Burak Y.V. & Teslyuk I.M. (2010) EPR spectroscopy of the Mn^{2+} and Cu^{2+} centres in lithium and potassium-lithium tetraborate glasses. *Acta Physica Polonica A*, **117**, 122–125.

Petra L., Billik P. & Komadel P. (2015) Preparation and characterization of hybrid materials consisting of high-energy ground montmorillonite and α-amino acids. *Applied Clay Science*, **115**, 174–178.

Ptáček P., Opravil T., Šoukal F., Havlica J., Másilko J. & Wasserbauer J. (2013) Preparation of dehydroxylated and delaminated talc: Meta-talc. *Ceramics International*, **39**, 9055–9061.

Ramadan A.R., Esawi A.M.K. & Gawad A.A. (2010) Effect of ball milling on the structure of Na^+-montmorillonite and organo-montmorillonite (Cloisite 30B). *Applied Clay Science*, **47**, 196–202.

Reddy S.L., Frost R.L., Sowjanya G., Reddy N.C.G., Reddy G.S. & Reddy B.J. (2008) EPR, UV-visible, and near-infrared spectroscopic characterization of dolomite. *Advances in Condensed Matter Physics*, 1–8.

Sanchez-Soto P.J., Wiewiòra A., Avilés M.A., Justo A., Pérez-Maqueda L.A., Pérez-Rodriguez J.L. & Bylina P. (1997) Talc from Puebla de Lillo, Spain. II. Effect of dry grinding on particle size and shape. *Applied Clay Science*, **12**, 297–312.

Siqueira R.E., Andrade M.M., Valezi D.F., Carneiro C.E. A., Pinese J.P.P., Costa A.C.S., Zaia D.A.M., Ralisch R., Pontuschka W.M., Guedes C.L.B. & Mauro E. (2011) EPR, FT-IR and XRD investigation of soils from Paraná, Brazil. *Applied Clay Science*, **53**, 42–47.

Solihin, Zhang Q.W., Tongamp W. & Saito F. (2010) Mechanochemical route for synthesizing $KMgPO_4$ and NH_4MgPO_4 for application as slow release fertilizers. *Industrial & Engineering Chemistry Research*, **49**, 2213–2216.

Solihin, Zhang Q.W., Tongamp W. & Saito F. (2011) Mechanochemical synthesis of kaolin–KH_2PO_4 and kaolin–$NH_4H_2PO_4$ complexes for application as slow release fertilizer. *Powder Technology*, **212**, 354–358.

Vizcayno C., Gutiérrez R.M., Castello R., Rodriguez E. & Guerrero C.E. (2010) Pozzolan obtained by mechanochemical and thermal treatments of kaolin. *Applied Clay Science*, **49**, 405–413.

Vyalikh A., Massiot D. & Scheler U. (2009) Structural characterisation of aluminium layered double hydroxides by ^{27}Al solid-state NMR. *Solid State Nuclear Magnetic Resonance*, **36**, 19–23.

Zhang Q.W., Solihin & Saito F. (2009) Mechanochemical synthesis of slow-release fertilizers through incorporation of alumina composition into potassium/ammonium phosphates. *Journal of the American Ceramic Society*, **92**, 3070–3073.